Cellular/Molecular

Retromer Binds the FANSHY Sorting Motif in SorLA to Regulate Amyloid Precursor Protein Sorting and Processing

Anja W. Fjorback,[1,5] Matthew Seaman,[2] Camilla Gustafsen,[1] Arnela Mehmedbasic,[1] Suzanne Gokool,[2] Chengbiao Wu,[3] Daniel Militz,[4] Vanessa Schmidt,[4] Peder Madsen,[1] Jens R. Nyengaard,[5] Thomas E. Willnow,[4] Erik Ilsø Christensen,[6] William B. Mobley,[3] Anders Nykjær,[1] and Olav M. Andersen[1]

[1]The Lundbeck Foundation Research Centre MIND, Department of Biomedicine, Aarhus University, DK-8000 Aarhus C, Denmark, [2]University of Cambridge, Cambridge Institute for Medical Research/Department of Clinical Biochemistry, Addenbrookes Hospital, Cambridge, CB2 0XY, United Kingdom, [3]University of California, San Diego, Department of Neurosciences, La Jolla, California 92093-0662, [4]Max Delbrueck Center for Molecular Medicine, 13125 Berlin, Germany, [5]MIND Centre, Stereology and Electron Microscopy Laboratory, Centre for Stochastic Geometry and Advanced Bioimaging, Aarhus University Hospital, DK-8000 Aarhus C, Denmark, and [6]Department of Biomedicine, Aarhus University, DK-8000 Aarhus C, Denmark

sorLA is a sorting receptor for amyloid precursor protein (APP) genetically linked to Alzheimer's disease (AD). Retromer, an adaptor complex in the endosome-to-Golgi retrieval pathway, has been implicated in APP transport because retromer deficiency leads to aberrant APP sorting and processing and levels of retromer proteins are altered in AD. Here we report that sorLA and retromer functionally interact in neurons to control trafficking and amyloidogenic processing of APP. We have identified a sequence (FANSHY) in the cytoplasmic domain of sorLA that is recognized by the VPS26 subunit of the retromer complex. Accordingly, we characterized the interaction between the retromer complex and sorLA and determined the role of retromer on sorLA-dependent sorting and processing of APP. Mutations in the VPS26 binding site resulted in receptor redistribution to the endosomal network, similar to the situation seen in cells with VPS26 knockdown. The sorLA mutant retained APP-binding activity but, as opposed to the wild-type receptor, misdirected APP into a distinct non-Golgi compartment, resulting in increased amyloid processing. In conclusion, our data provide a molecular link between reduced retromer expression and increased amyloidogenesis as seen in patients with sporadic AD.

Introduction

Elevated production of the amyloid β (Aβ) peptide is widely accepted as a neurotoxic event in Alzheimer's disease (AD) (Haass and Selkoe, 2007). Aβ is generated by sequential enzymatic cleavages of amyloid precursor protein (APP) by β- and γ-secretases. In an alternative non-amyloidogenic pathway, APP is processed by the α-secretase enzyme that clips within the Aβ peptide, thereby precluding amyloid formation. Increasing evidence suggests that intracellular APP trafficking determines the access of APP to the respective secretases and thereby regulates the balance between amyloidogenic and non-amyloidogenic processing (Sannerud and Annaert, 2009). Thus, dissecting the APP trafficking pathway is of critical importance for understanding how Aβ is formed.

sorLA (alternatively named LR11 or SORL1) is a 250 kDa member of the VPS10p-domain receptor family of type-1 sorting receptors (Willnow et al., 2008). We and others have shown that sorLA binds APP and retains it in the Golgi compartment, thereby preventing processing of the precursor into Aβ (Andersen et al., 2005, 2006; Offe et al., 2006; Schmidt et al., 2007; Dodson et al., 2008; Rohe et al., 2008). Accordingly, single nucleotide polymorphisms in *SORL1*, the gene encoding sorLA, are associated with late-onset AD, and sorLA expression is reduced in vulnerable brain regions of AD patients (Scherzer et al., 2004; Andersen et al., 2005; Dodson et al., 2006; Rogaeva et al., 2007).

Although the significance of sorLA for controlling APP transport and processing is well appreciated, little is known about the molecular mechanisms that guide the receptor through the intracellular compartments. Trafficking of sorLA is likely to be regulated by a complex system of cytoplasmic adaptor proteins that bind to specific target sequences within the cytoplasmic tail of the receptor. This assumption is supported by the observation that VPS10p, the yeast homolog of sorLA, requires the retromer complex for proper sorting (Seaman et al., 1997, 1998). In mammals, retromer is composed of at least five different proteins arranged in two subcomplexes comprising VPS26, VPS29, and VPS35 (the VPS trimer) and a dimer of two sorting nexin proteins (SNX1 or SNX2 with SNX5 or SNX6) (Seaman, 2005; Wassmer et al.,

Received May 6, 2011; revised Sept. 30, 2011; accepted Nov. 28, 2011.

Author contributions: A.W.F., M.S., T.E.W., A.N., and O.M.A. designed research; A.W.F., M.S., C.G., A.M., S.G., C.W., D.M., P.M., E.I.C., and O.M.A. performed research; V.S., J.R.N., and W.B.M. contributed unpublished reagents/analytic tools; A.W.F., M.S., C.G., S.G., C.W., D.M., P.M., T.E.W., E.I.C., A.N., and O.M.A. analyzed data; A.W.F., M.S., T.E.W., A.N., and O.M.A. wrote the paper.

This research was funded by The Lundbeck Foundation, Alzheimer's Association Grant NIRG-08-89450, The Novo Nordic Foundation, Alzheimerforskningsfonden, The Carlsberg Foundation, The Augustinus Foundation, The Villum Foundation, The Danish Medical Research Council, and The Aase and Ejnar Danielsen Foundation. M.S. is funded by a Senior Research Fellowship Award from the Medical Research Council. We thank Drs. Bent Honoré (Aarhus University, Aarhus, Denmark) and Robin Antrobus (Cambridge Institute for Medical Research, Cambridge, UK) for mass spectrometry analysis and Jana Zenker, Marit Nielsen, Michelle Leganger, Anja Aagaard, Hanne Sidelmann, Inger B. Kristoffersen, and Anne Marie Bundsgaard for expert technical assistance.

The authors disclose no conflicts of interest.

Correspondence should be addressed to Dr. Olav M. Andersen, MIND Centre, Department of Biomedicine, Ole Worms Alle 3, Building 1170, Aarhus University, DK-8000 Aarhus C, Denmark. E-mail: o.andersen@biokemi.au.dk.

DOI:10.1523/JNEUROSCI.2272-11.2012

 0270-6474/12/321467-14$15.00/0

2007). The cargo binding activity of retromer is assigned to the VPS trimer, and, in all cases in which this has been studied, binding is mediated by the VPS35 subunit (Collins, 2008).

The retromer complex is essential for normal cellular function, as illustrated by the embryonic lethality of knock-out mice devoid in VPS26 or in SNX1 and SNX2 expression (Lee et al., 1992; Schwarz et al., 2002). Previous studies have also suggested that retromer is engaged in binding and trafficking of the mammalian sorLA protein (Lane et al., 2010) because knockdown of either VPS35 or SNX1 results in reduced sorLA expression (Nielsen et al., 2007).

Similarly to sorLA, expression of the retromer component VPS35 is decreased in vulnerable regions of AD brains, but the mechanism by which retromer influences onset of disease remains poorly understood (Small et al., 2005). However, recent studies reported that retromer deficiency in mice and flies increases the production of Aβ (Muhammad et al., 2008), likely by impact on APP sorting (Vieira et al., 2010). Because the retromer complex does not interact directly with APP, we speculated that sorLA is the molecular link between retromer function and APP processing. We provide evidence for a direct link between sorLA and retromer and suggest a model on how they jointly prevent APP from entering the amyloidogenic pathway.

Materials and Methods

Antibodies. Antibodies used against the following antigens are listed with their source followed by the dilution factor for Western blot (WB) or immunofluorescence (IF) applications. Actin (Sigma; WB, 1:1000), APP C-terminal (O.M.A.; WB, 1:1000; IF, 1:300), APP/8E5 (B. T. Hyman, Massachusetts General Hospital, Cambridge, MA; IF, 1:300), sol–sorLA from rabbit, goat, or mouse (C. M. Petersen, Aarhus University, Aarhus, Denmark; WB, 1:1000; IF, 1:300), CD8 (Santa Cruz Biotechnology; WB, 1:200; M.S.; IF, 1:200), β1-adaptin: (a gift from M. S. Robinson, University of Cambridge, Cambridge, UK; WB, 1:1000), Mannosidase II (ManII) (Millipore Bioscience Research Reagents; IF, 1:300), sAPPα/WO2 (R. Cappai, The University of Melbourne, Melbourne, Australia; WB, 1:2000), TGN46 (M.S.; IF, 1:300), VPS26 (M.S.; IF, 1:300), VPS35 (M.S.; IF, 1:300), Snx1 (M.S.; IF, 1:300), and TGN38 (M.S.; IF, 1:300). As secondary antibodies, we used Alexa Fluor donkey anti-rabbit 488, 546, 555, or 568, Alexa Fluor donkey anti-mouse 488, and Alexa Fluor donkey anti-goat 568 or 546 (all from Calbiochem/Invitrogen; IF, 1:300).

DNA constructs and recombinant proteins. The construct encoding the full-length sorLA–FANSHY→6A mutant was generated by site-directed mutagenesis of the human sorLA cDNA in pcDNA3.1zeo(+) vector using primers 5-GCA GCT TCA CCG CCG CTG CCG CAG CGG CAG CTA GCT CCA GGC-3 and 5-GGC AAC TAG AAG GCA CAG TCG AGG-3, and, accordingly, 5-GCC TGG AGC TAG CTG CCG CTG CGG CAG CGG CGG TGA AGC TGC-3 and 5-CTT GCA AAC GTC ACT GCT GCC TCC-3. The wild-type (WT) sorLA fragment was replaced by the mutated PCR fragment via SfuI and XhoI. The CD8^{ED}–sorLA^{CD}–WT construct was made as described previously (Seaman, 2004), involving PCR amplification of the cytoplasmic tail of WT sorLA and adding an AflII site to form an in-frame fusion with human CD8α. Thus, the cytoplasmic domain of sorLA was joined to the lumenal domain of CD8α. Site-directed mutagenesis of the sorLA tail was accomplished using the QuikChange kit by Stratagene, following the instructions of the manufacturer.

H6Ubi-tail proteins were produced in *Escherichia coli* BL21/DE3 pLysS as described previously (Andersen et al., 2000). Expression constructs were prepared using the following forward and reverse primers: 5′-GGC GGA TCC ATC GAG GGT AGG TAC ACG AAG CAC CGG AGG CTG CAG AGC AGC-3′ and 5′-CGG TTC GAA TTC AGG CTA TCA CCA TGG GGA CGT CAT CTG-3′. Bacterial cells were lysed and applied to an Ni^{2+}-charged NTA column equilibrated with 50 mM Tris-HCl, pH 8.0, and 500 mM NaCl. Bound protein was eluted by addition of 20 mM EDTA. The quality of the H6Ubi-tail proteins was tested by SDS-PAGE analysis.

The human VPS26A protein (GenBank accession number NP_004887) was expressed with a C-terminal histidine tag by using the pET11a vector (Novagen) and purified from *E. coli* lysate on Talon beads (Invitrogen). The GGA1–VHS domain was produced as described previously (Cramer et al., 2010).

A vector for short-hairpin RNA (shRNA) knockdown of VPS26 was prepared based on the siRNA sequence against VPS26 (AAU GAU GGG GAA ACC AGG AAA), the BLOCK-iT Inducible H1 RNAi Entry Vector kit (Invitrogen), and a pair of oligonucleotides. The oligos used were as follows: 5′-CACC AAT GAT GGG GAA ACC AGG AAA GAGA TTT CCT GGT TTC CCC ATC ATT-3′ (top strand) and 5′-AAAA AAT GAT GGG GAA ACC AGG AAA TCTC TTT CCT GGT TTC CCC ATC ATT-3′ (bottom strand).

APP metabolism. SH-SY5Y cells were cultured in DMEM F-12 (Invitrogen) supplemented with 10% FBS and 5% penicillin/streptomycin. To obtain stable cell lines, SH-SY5Y cells were transfected using HiFect (Amaxa) with constructs encoding sorLA–WT or sorLA–FANSHY→6A. Transfected cells were selected by adding 300 μg/ml zeocin (Invitrogen) to the medium 48 h after transfection. Determination of APP metabolism was performed using the endogenous level of APP expression in the stable transfected SH-SY5Y cells. A total of 5×10^6 cells were cultured in T25 flasks (Nunc) and allowed to grow to >90% confluency before shifting the medium to serum-free DMEM F-12. Both medium and cells were harvested after another 45 h. Cells were lysed using 10 mM Tris-HCl, pH 8, 5 mM EDTA, 1% Triton X-100, and 1% NP-40. Equal amounts of protein from cells and medium were suspended in SDS loading buffer and loaded onto 4–16% SDS-PAGE, followed by WB. The nitrocellulose membranes (GE Healthcare) were probed for sorLA, holo-APP, and actin. The Aβ_{1-40} level was determined by ELISA (Invitrogen).

Cell surface biotinylation. SH-SY5Y cell lines stably expressing either sorLA–WT or sorLA–FANSHY→6A were grown in six-well plates and used at 80% confluency. Cells were washed twice with ice-cold PBS and incubated for 30 min on ice with PBS containing 1 mg/ml EZ-linked sulfo-NHS-S-biotin (Pierce). Biotinylation was quenched by 20 min of incubation with 100 mM glycine. The quenching buffer was removed by washing in PBS, and the cells were lysed in lysis buffer (PBS, 1% Triton X-100, and 0.1% SDS) supplemented with Complete proteinase inhibitor (Roche). To precipitate the biotinylated proteins, cell lysates were incubated with streptavidin beads (GE Healthcare) overnight at 4°C. After incubation, the beads were washed three times in PBS before being eluted with 50 μl of SDS sample buffer and incubated at 98°C for 5 min. The total protein fraction (20 μg of sorLA–WT or sorLA–FANSHY→6A) and the cell surface fraction (20 μl of sorLA–WT and sorLA–FANSHY→6A) were loaded onto SDS-PAGE (4–16%), followed by WB. The membrane was probed with antiserum against sol–sorLA.

Protein lifetime and maturation. A pulse-chase experiment was performed using 1.5×10^6 of SH-SY5Y cells stably expressing sorLA–WT or sorLA–FANSHY→6A. The cells were incubated in cysteine and methione-free medium (Sigma) for 15 min before metabolic labeling [200 μCi/ml L-[^{35}S]cysteine and L-[^{35}S]methione (Pro-mix; GE Healthcare) in the presence of 1× Glutamax (Sigma)] for 40 min. Thereafter, the cells were washed in PBS and incubated in complete DMEM and chased for the indicated times, followed by cell lysis. sorLA–WT and sorLA–FANSHY→6A were immunoprecipitated using Gamma-bind Sepharose beads (GE Healthcare) coated with rabbit serum against sol–sorLA. The precipitated proteins were analyzed by SDS-PAGE, followed by autoradiography.

As described previously (Seaman, 2007), determination of the CD8^{ED}–sorLA^{CD}–WT and mutant stability was performed in the presence of cycloheximide, except that the cells were grown in 90 mm tissue culture dishes and were treated with cycloheximide for 4 h.

Confocal microscopy. With the purpose of studying colocalization of sorLA with different marker proteins, we used primary hippocampal neuronal cultures and human SH-SY5Y cell lines stably expressing either sorLA–WT or sorLA–FANSHY→6A. Furthermore, we used SH-SY5Y cells transiently transfected with either CD8^{ED}–sorLA^{CD}–WT or CD8^{ED}–sorLA^{CD}–FANSHY→6A in combination with sorLA–WT, sorLA–FANSHY→6A, sorLA–F^{12}→A, sorLA–FTAF→4A, and sorLA–Y^{17}→F. The following procedure was used in connection with all cell

staining experiments unless otherwise stated. The cells were fixed in 4% paraformaldehyde for 10 min, after which the paraformaldehyde was removed by washing three times in PBS. The cells were then permeabilized for 30 min by incubation in PBS containing 0.1% Triton X-100. Next, cells were blocked for 30 min in blocking buffer [PBS containing 10% fetal calf serum (FCS)]. After blocking, the cells were incubated with primary antibodies diluted in blocking buffer for 2 h at room temperature or overnight at 4°C. The cells were then washed three times in PBS and incubated with secondary antibodies for 2 h at room temperature in the dark. The cells were imaged using a Carl Zeiss confocal LSM 510 META laser microscope with 40×, NA 1.2 C-Apochromat objectives (Carl Zeiss).

Endosome-to-Golgi retrieval of CD8^{ED}–sorLA^{CD}–WT and CD8^{ED}–sorLA^{CD}–FTAF→4A was investigated using the antibody-uptake assay as described previously (Seaman, 2004, 2007). In this assay, cells expressing the CD8-reporter construct of interest were incubated with anti-CD8 antibody continuously for 3 h. After fixation, the cells were permeabilized and labeled with anti-TGN46 antisera and then fluorescently labeled with anti-mouse and anti-rabbit secondary antibodies. The cells were imaged as described previously (Seaman, 2007).

Live-cell imaging. PC12 cells were maintained in DMEM (4.5 mg/L glucose) supplemented with 10% horse serum and 5% fetal bovine serum. Cells were incubated at 37°C with 5% CO_2. The plasmid containing mCherry and GFP-tagged APP or sorLA were transfected into 70–80% confluent PC12 cells using Lipofectamine 2000 (Invitrogen). The day after transfection, the cells were seeded onto coverslips coated with Matrigel (BD Biosciences). The cells were incubated in serum-free medium supplemented with NGF (50 ng/ml) 24–48 h before investigation. The cells were investigated using a Nikon E800 epifluorescence microscope, and images were captured using a CCD camera. Movies were generated by obtaining images at 1 frame/s with a 100× oil-immersion objective (NA 1.4). The vesicle movement was analyzed by generation of kymostacks using a homemade NIH ImageJ KymoToolbox plugin (http://rsb.info.nih.gov/ij/; available on request at Fabrice.Cordelieres@curie.fr). A number of vesicles was analyzed per condition (APP, 354 vesicles; sorLA–WT, 226 vesicles; sorLA–FANSHY→6A, 287 vesicles) over three experiments ($n = 3$).

Fluorescence lifetime imaging microscopy (FLIM) was conducted to determine FRET between APP and either sorLA–WT or the sorLA–FANSHY→6A mutant. The FLIM experiments of the cells were investigated on a Carl Zeiss confocal LSM 510 META laser microscope with a 40×, NA 1.2 C-Apochromat objective. This microscope is equipped with a mode-locked titanium–sapphire two-photon laser (Mai-Tai; Spectra Physics), photon counting card (SPC830), and associated software from Becker & Hickl (SPCM program). APP was detected with antibody 8E5 and anti-rabbit labeled with Alexa Fluor 488. Alexa Fluor 488 fluorescence was detected with a PMC-100 detector (Hamamatsu) after two-photon excitation at 800 nm. Images in the SPCM program were 256 × 256 pixels in size and 256 time channels in depth, and they were acquired with the following settings in the LSM program: pixel dwell time, 1.6 μs; line average, 1 and 0.11 μm/pixel (zoom 4).

Fluorescence lifetime decay curves were collected in 10 cycles of 10 s. Lifetimes were measured for APP labeled with Alexa Fluor 488 in the presence and absence of sorLA–WT or sorLA–FANSHY→6A labeled with Alexa Fluor 543, respectively. Lifetime curves were obtained from 10–15 cells. The fluorescence decay curves were fitted to a monoexponential decay function in SPCImage (Becker & Hickl, version 2.9.4.1993) with bin set to 1 (3 × 3 pixels) and amplitude threshold set to 25. The scatter parameter was fixed to 0, and all other parameters were left free. As instrument response function, we used the one automatically calculated by SPCImage.

Proximity ligation assay. According to protocol (Söderberg et al., 2006), the localization and interactions between endogenous APP and sorLA–WT or the sorLA–FANSHY→6A mutant were analyzed using a proximity ligation assay (PLA). SH-SY5Y cells transfected with sorLA–WT or sorLA–FANSHY→6A were fixed on coverslips with 4% paraformaldehyde, and membranes were permeabilized with 0.5% saponin. The cells were incubated overnight at 4°C with mouse anti-sorLA (20C11) and rabbit anti-APP (C terminal). After washing three times, the cells were incubated with secondary antibodies conjugated with oligonucleotides: PLUS-anti-rabbit PLA probe and MINUS-anti-mouse PLA probe, respectively. In the following steps, the PLUS and the MINUS probes in close proximity (<40 nm) were hybridized and ligated. The interacting probes were then amplified with polymerase. DNA strands were visualized by hybridization of fluorescently labeled oligonucleotides and analyzed by fluorescence microscopy (563 nm). All incubations were done at 37°C using the incubation times and buffers given by the manufacturer (Olink Bioscience).

CD8 native immunoprecipitations (IPs) were performed as described previously (Seaman, 2007). Cells were grown in 140 mm dishes and lysed in 1 ml of lysis buffer (0.1 M Mes-NaOH, pH 6.5, 1 mM Mg-acetate, 0.5 mM EGTA, 200 μM Na-vanadate, 1% digitonin, and protease inhibitors). The cell lysate was centrifuged for 5 min at 10,000 × *g*, after which the supernatant was cleared by incubation with 50 μl of protein-A Sepharose (25%) for 30 min at 4°C. The lysates were then centrifuged again for 5 min at 10,000 × *g* and, subsequently, transferred to a fresh tube containing ~5 μg of anti-CD8 prebound to protein-A Sepharose. After 90 min of incubation at 4°C, the IPs were washed four times with lysis buffer. Next, the samples were desiccated in a Speed-Vac, resuspended into 50 μl of SDS-PAGE loading buffer, and subjected to SDS-PAGE and WB analysis.

Large-scale anti-CD8 native IPs were performed as above using six 140 mm dishes of cells for each CD8 reporter. After washing, the IPs were combined into a spin column (one column per CD8 reporter), and the bound proteins were eluted using 2 × 150 μl aliquots of 200 mM glycine-HCl, pH 2.3. After elution, the proteins were precipitated by addition of 1.2 ml of ice-cold acetone. After precipitation with acetone, the precipitated proteins were dried in a Speed-Vac and then prepared for liquid chromatography with tandem mass spectrometry analysis as described previously (Harbour et al., 2010).

Peptide pull-downs and mass spectrometry. Peptides containing the cytosolic tail of human sorLA were purchased from Eurogentec and dissolved in ultra-pure water (1 mg of peptide in 200 μl of H_2O). Peptide 1 was soaked in 4 μl of DMSO before dissolving in water. According to the SulfoLink manual (Pierce), the peptides were then coupled to iodoacetyl-activated agarose (SulfoLink Coupling Resin; Pierce). As a control for unspecific resin binding, one batch of beads was treated in parallel but without addition of the peptide. The binding efficiency was estimated by applying a BCA assay on the peptide solution before and after coupling to the Sepharose. A >90% decrease in signal (and a decrease of peptide in solution therewith) was considered as efficient coupling. After the coupling, free binding sites were blocked by 50 mM cysteine.

Animals were killed, and kidneys were removed rapidly, rinsed briefly in PBS, and homogenized with an Ultra-Turrax (IKA) in 1 ml of ice-cold RIPA buffer (0.2% SDS, 0.1% sodium deoxycholate, 1% NP-40, 150 mM NaCl, 50 mM Tris-HCl, 2 mM 2-mercaptoethanol, and 5 mM EDTA, pH 7.4) or DOC buffer (10% sodium deoxycholate and 500 mM Tris-HCl, pH 7.4) per 50 mg of tissue. The homogenates were incubated on ice for 10 min before they were sonicated. To enrich cytosolic proteins, the lysate was cleared by centrifugation at 126.200 × *g* for 30 min at 4°C. Protein concentrations were estimated by performing a BCA assay (with comparison with a BSA standard). One milligram of protein was incubated overnight at 4°C with 50 μl of settled peptide-coupled resin. Next, the column was washed five times for 5 min with 1 ml of either RIPA or DOC buffer. Bound proteins were eluted by incubating the beads in 20 μl of 4× SDS-PAGE sample buffer (200 mM Tris-HCl, 8% SDS, 0.04% bromophenol blue or orange G, 40% glycerol, and 200 mM 2-mercaptoethanol, and pH 6.8) at 95°C for 5 min. The samples were subjected to SDS-PAGE and stained with Coomassie blue G250 (Sigma-Aldrich). The bands of interest were excised, and the gel pieces were stored at 4°C in 1% acetic acid. Mass spectrometry (MS) for protein/peptide identification was performed by Gunnar Dittmar (Max Delbrueck Center, Berlin, Germany), Heike Stephanowitz (Leibniz Institute for Molecular Pharmacology, Berlin, Germany), or Bent Honoré (Aarhus, Denmark).

Surface plasmon resonance analysis. As described previously (Andersen et al., 2006), immobilization of H6Ubi–sorLA–WT and H6Ubi–sorLA–FANSHY→6A was performed after dialysis against sodium acetate, pH 4.0 and coupled to CM5 chips (BIAcore). The sample and running buffer

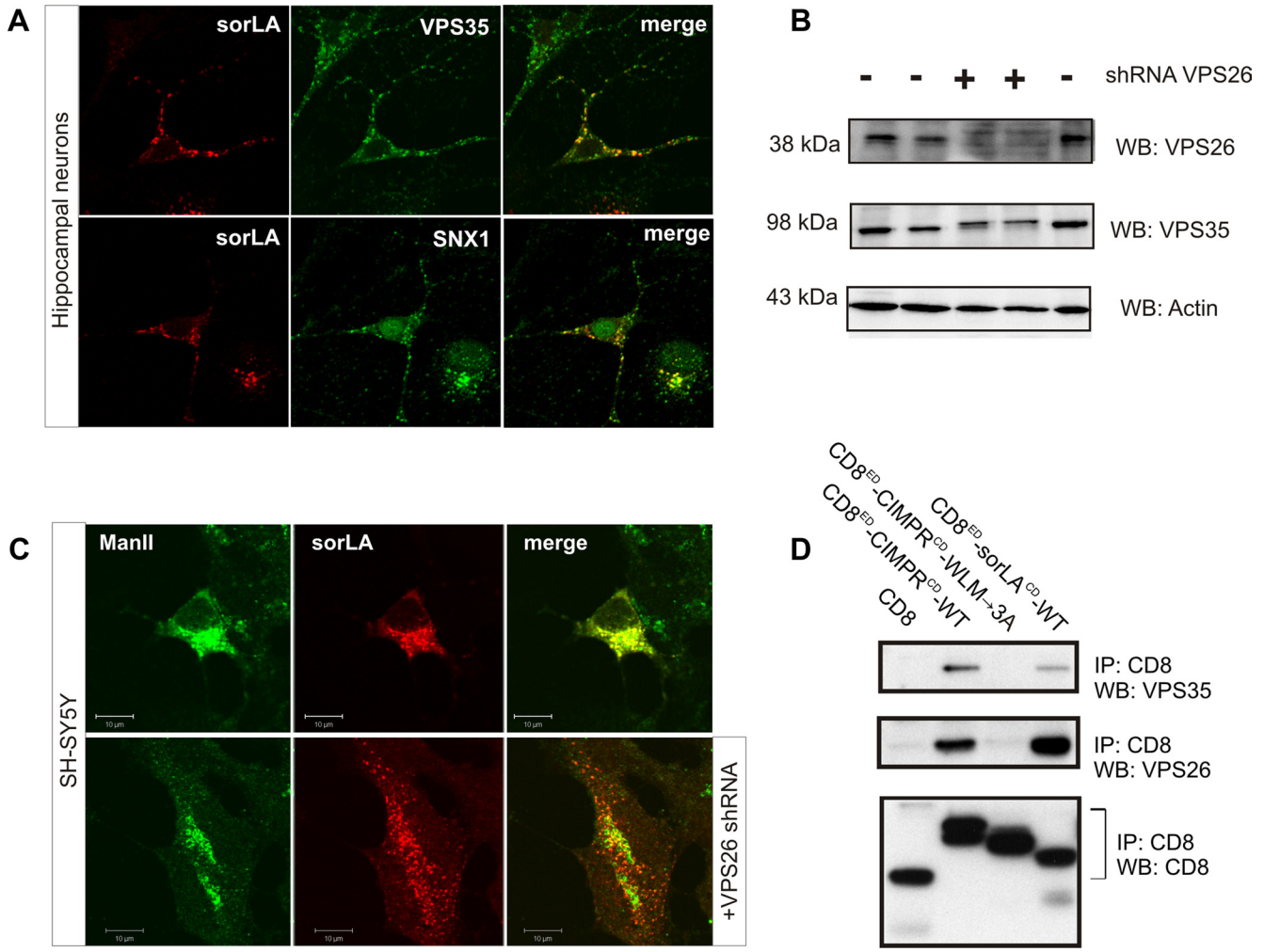

Figure 1. Retromer physically interacts with sorLA. ***A***, Immunostaining of primary hippocampal neurons for sorLA (red) and VPS35 (in green; top) or SNX1 (in green; bottom). ***B***, WB analysis of lysates from SH-SY5Y cells after transfection with (+) or without (−) an shRNA vector against human VPS26. Actin is used as loading control. ***C***, SH-SY5Y cells were transfected with sorLA–WT (top) or sorLA–WT together with the VPS26 shRNA knockdown vector (bottom) sorLA (red) and the Golgi marker ManII (green). ***D***, Co-IP analysis of CD8 chimeric proteins as previously (reported by Skinner and Seaman, 2009). Precipitated proteins were analyzed by WB.

used for binding analysis were 10 mM HEPES, pH 7.4, 150 mM NaCl, 3 mM EGTA, and 0.005% Tween 20. The regeneration of the chip was performed by alternating 10 μl pulses of regeneration buffer (10 mM glycine hydrochloride, pH 4.0, 20 mM EDTA, 500 mM NaCl, and 0.005% Tween 20) and 0.01% SDS. All measurements were conducted on a BIAcore3000 instrument.

Immunoelectron microscopy. For electron microscopy, cells were fixed with 2% formaldehyde and 0.1% glutaraldehyde in 0.01 M PBS, pH 7.4, for 10 min at room temperature. The cells were washed three times and removed with a rubber policeman in the same buffer containing 1% gelatin (Merck). The cells were then pelleted and embedded in 12% gelatin, infiltrated with 2.3 M sucrose in PBS for 30 min, and, finally, frozen in liquid nitrogen. Ultrathin cryosections (70 ± 90 nm) were obtained with an FCS Reichert Ultracut S cryo-ultramicrotome at −100°C and collected on 200 mesh nickel grids. The sections were incubated overnight with a polyclonal rabbit anti-sol–sorLA antibody at 1:1000 before 2 h of incubation with goat anti-rabbit gold (10 nm) (BioCell). All incubations were performed at 4°C. Finally, the sections were contrasted with methyl cellulose containing 0.3% uranylacetate and studied in a Philips CM100 electron microscope.

Results

Retromer binds and regulates the localization of sorLA

Expression of sorLA and retromer has been detected previously in a subset of neuronal cells within the mammalian brain. To determine whether these proteins colocalize, we performed immunostaining for sorLA and the retromer proteins VPS35 and SNX1 in primary hippocampal cultures. We observe that sorLA and the two retromer proteins partly overlap in a perinuclear compartment (Fig. 1*A*). Noticeably, not all cells stained for sorLA, which is in line with the previously shown heterogeneous cellular pattern of sorLA immunostaining of brain, including hippocampus (Motoi et al., 1999).

Based on the colocalization seen in hippocampal neurons, we decided to investigate whether the retromer complex regulates the intracellular distribution of sorLA. For that purpose, we prepared a shRNA knockdown vector against the human VPS26 protein and transfected the construct into SH-SY5Y cells to test for its ability to reduce VPS26 expression. As seen by WB, VPS26 and VPS35 protein expression were clearly visible in nontransfected cells. However, VPS26 was undetectable in cells transfected with the shRNA vector (Fig. 1*B*). We also found that the level of VPS35 was decreased in VPS26-depleted cells. This observation is in agreement with previous studies showing that VPS proteins of the cargo-selective subcomplex stabilize each other (Arighi et al., 2004; Seaman, 2004) (Fig. 1*B*).

We next performed confocal fluorescence microscopy to investigate whether retromer deficiency changes the subcellular lo-

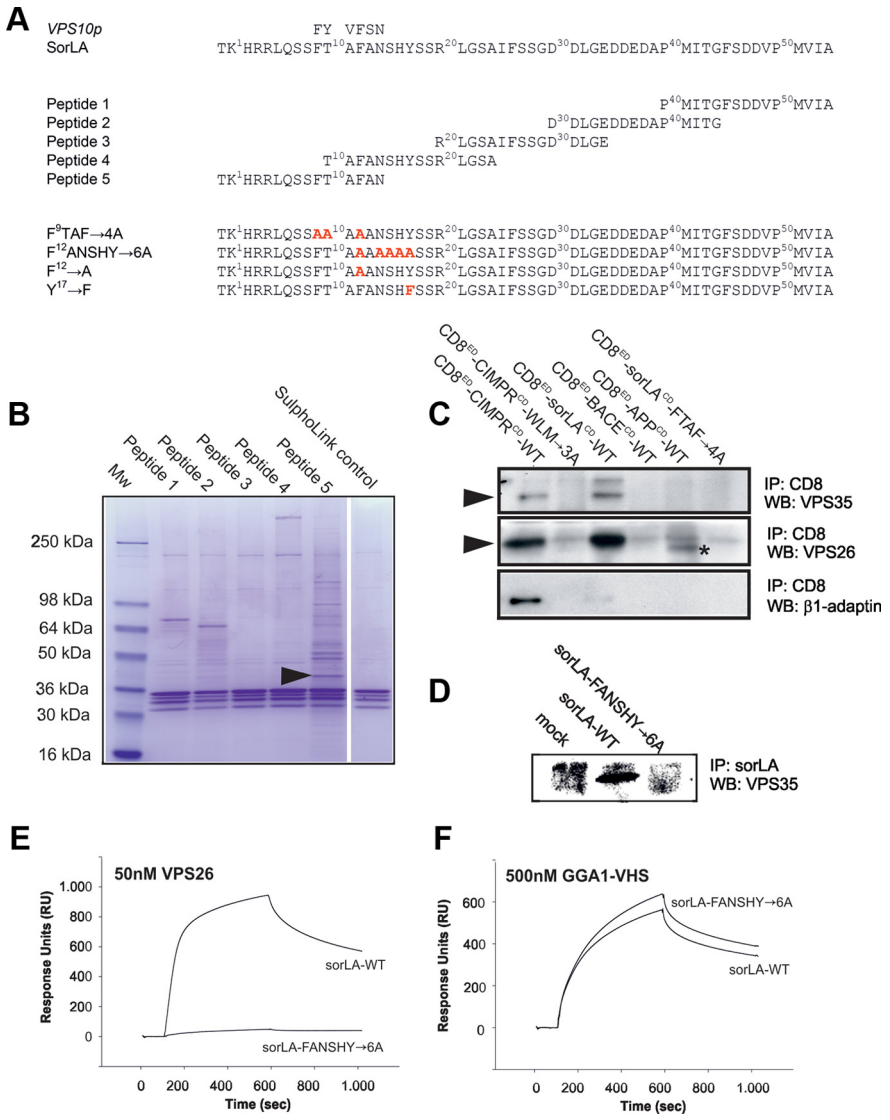

Figure 2. Aromatic residues in sorLA are important for the association with retromer proteins. ***A***, Amino acid sequences of human WT and mutant sorLA cytoplasmic tails. Overlapping 15-mer peptides used for pull-down studies are indicated. ***B***, Precipitated proteins are visualized by SDS-PAGE and Coomassie staining. The arrowhead marks the VPS26 subunit identified by MS in several independent experiments. ***C***, Co-IP analysis of CD8 chimeric proteins from transfected HeLa cells. Precipitated proteins were analyzed by WB. The asterisk in lane CD8^{ED}–APP^{CD}–WT indicates an unknown protein unrelated to VPS26. ***D***, Co-IP of VPS35 with sorLA–WT from stably transfected SH-SY5Y cells. ***E***, ***F***, Surface plasmon resonance analysis using 50 nM VPS26 protein or 500 nM GGA1–VHS domain applied to biosensor surfaces immobilized with sorLA–WT and sorLA–FANSHY→6A tails fused to H6Ubi.

calization of sorLA. SH-SY5Y cells were transfected with an expression vector for sorLA alone or cotransfected with the VPS26 shRNA knockdown vector. In the presence of functional retromer in single-transfected SH-SY5Y cells, sorLA was observed within the perinuclear region showing strong overlap with the Golgi marker ManII. However, in the retromer knockdown cells (i.e., double-transfected cells), the receptor displayed a more punctate and peripheral distribution (Fig. 1*C*). This change in sorLA localization suggests that retromer acts in the retrieval of sorLA from a peripheral compartment (e.g., early and/or recycling endosomes) to the Golgi.

Because knockdown of VPS26 alters sorLA distribution, we wanted to examine whether sorLA and retromer can physically interact. We therefore performed co-IP experiments using a chimeric reporter construct encoding the extracellular domain (ED) of CD8 fused to the cytoplasmic domain (CD) of sorLA (CD8^{ED}–sorLA^{CD}–WT). Because previous reports described that the retromer complex associates with the cytoplasmic tail of the cation-independent mannose 6-phosphate receptor (CIMPR), we used a CD8^{ED}–CIMPR^{CD}–WT fusion construct as a positive control. As negative control, we applied CD8 alone or a mutated variant (CD8^{ED}–CIMPR^{CD}–WLM→3A) lacking the retromer binding site (Seaman, 2007). IP experiments were performed on lysates from transfected HeLa cells using an anti-CD8 antibody. As shown in Figure 1*D*, the retromer proteins VPS35 and VPS26 coprecipitated with CD8^{ED}–sorLA^{CD}–WT and CD8^{ED}–CIMPR^{CD}–WT but not with CD8^{ED}–CIMPR^{CD}–WLM→3A or CD8 alone. These data provide evidence that retromer and sorLA physically associate within cells (Fig. 1*D*).

Identification of the retromer binding motif in sorLA

To identify the retromer binding site in sorLA, we prepared overlapping 15-mer peptides corresponding to the cytoplasmic tail (sorLA peptides 1–5; Fig. 2*A*) and coupled these peptides to Sepharose resin. The peptides were then incubated with homogenates of mouse kidney—a tissue shown to contain high levels of retromer and sorLA (Reiche et al., 2010 and data not shown)—and bound proteins were eluted and analyzed by SDS-PAGE, followed by Coomassie staining. Prominent bands were subsequently identified by MS. Interestingly, we noticed that peptide 5 covering the sequence closest to the transmembrane domain of sorLA bound several proteins, including VPS26 (Fig. 2*B*). Notably, peptide 5 is rich in aromatic residues, including the di-phenylalanine motif FTAF (Fig. 2*A*). This sequence is similar to the FYVF motif in the yeast VPS10p receptor that is believed to mediate binding to the yeast retromer complex (for review, see Seaman, 2008).

To test whether the aromatic residues present in peptide 5 are involved in retromer binding, we mutated the FTAF motif within the CD8^{ED}–sorLA^{CD}–WT to a tetra-alanine sequence (CD8^{ED}–sorLA^{CD}–FTAF→4A). We then repeated the co-IP experiment in HeLa cells, comparing retromer precipitation for CD8^{ED}–sorLA^{CD}–WT and CD^{ED}–sorLA^{CD}–FTAF→4A (Fig. 2*C*). We found that both VPS26 and VPS35 associated with the chimeric protein carrying the WT sorLA tail sequence (Fig. 2*C*). However, when the cytoplasmic FTAF motif was mutated, the interaction with retromer was abolished (Fig. 2*C*). Additionally, β1-adaptin, a component of the clathrin AP-1 complex, showed specific interaction with CD8^{ED}–CIMPR^{CD}–WT but did not bind to sorLA. Notably, neither the tail of APP nor of the β-site APP-cleaving enzyme (BACE) could precipitate components of the retromer in this assay (Fig. 2*C*).

Table 1. MS analysis of anti-CD8 native IP assays from HeLa cell lysates using CD8 reporter proteins

Protein detected	$CD8^{ED}$–$CIMPR^{CD}$–WT	$CD8^{ED}$–$sorLA^{CD}$–WT	$CD8^{ED}$–$sorLA^{CD}$–FANSHY→6A
β1-Adaptin	714 (14)	0	0
γ-Adaptin	434 (9)	30 (1)	0
μ1-Adaptin	330 (7)	0	0
GGA2	0	46 (1)	0
VPS35	79 (5)	426 (7)	27 (1)
VPS26A	0	26 (1)	0
VPS29	0	39 (1)	0
SNX2	51 (2)	0	0
SNX6	150 (1)	0	0
Rab7A	36 (1)	22 (1)	26 (1)
CD8α	1783 (6)	1425 (5)	188 (4)
GAPDH	444 (6)	93 (4)	407 (4)
EF1A1	579 (6)	394 (5)	353 (5)
TfnR	424 (12)	1982 (13)	184 (8)

Immunoprecipitates of cells stably expressing the indicated CD8-reporter construct using an antibody against CD8. Values indicate the Mascot score and numbers in parentheses the quantity of peptides detected. The data are based on searching the MaxQuant database.

Phenylalanine residue 12 (F^{12}; numbering according to the tail sequence in Fig. 2*A*) is also part of an F*X*NP*X*Y-like motif known to function in the clathrin-dependent endocytosis pathway [i.e., for the low-density lipoprotein receptor (Davis et al., 1986)]. Therefore, we prepared a sorLA mutant wherein the FANSHY hexa-peptide was substituted with six alanine residues. SH-SY5Y cells were transfected with either sorLA–WT or sorLA–FANSHY→6A constructs, and co-IP of the retromer was performed. Because co-IP of VPS35 was only seen for cells that expressed sorLA–WT (Fig. 2*D*), we conclude that aromatic residues in sorLA are essential for binding the retromer complex.

To further investigate the binding partners of the cytoplasmic domain of sorLA, we applied a large-scale IP assay using HeLa cells stably transfected with the $CD8^{ED}$–$CIMPR^{CD}$–WT, $CD8^{ED}$–$sorLA^{CD}$–WT, and $CD8^{ED}$–$sorLA^{CD}$–FANSHY→6A mutant reporter constructs, respectively. Proteins immunoprecipitated with anti-CD8 antibodies were subsequently analyzed by MS. As shown in Table 1, peptides from the clathrin adaptor AP-1 (adaptins) were detected in the $CD8^{ED}$–$CIMPR^{CD}$–WT sample, along with peptides from the retromer protein VPS35. The $CD8^{ED}$–$sorLA^{CD}$–WT sample contained peptides from VPS35, VPS26, and VPS29, but only one peptide from VPS35 was detected in the $CD8^{ED}$–$sorLA^{CD}$–FANSHY→6A sample. Similar numbers of peptides from the CD8α protein, GAPDH, and elongation factor were present in all three samples, indicating that comparable amounts of material were analyzed from each sample (Table 1). Next, we measured whether recombinant VPS26 can interact directly with the 54 aa tail of sorLA using surface plasmon resonance analysis. Whereas the nonmutated cytoplasmic part of sorLA bound strongly to VPS26, the tail of sorLA–FANSHY→6A failed to do so (Fig. 2*E*). However, both proteins bound to the GGA1 VHS domain shown previously to interact in a region that shares no overlap with the FANSHY motif (Nielsen et al., 2001; Cramer et al., 2010) showing a specific disruption of the VPS26 binding site (Fig. 2*F*).

Together, these data demonstrated that sorLA binds the VPS26 subunit of retromer and suggest that this interaction requires aromatic residues in the receptor tail.

Lack of retromer binding alters the localization of sorLA–FANSHY→As

We next investigated the effect of mutating the FANSHY sequence on cellular distribution of sorLA. In this assay, SH-SY5Y cells were double transfected with different combinations of CD8-reporter and full-length sorLA constructs to analyze the localization pattern of both proteins within the same cell. First, we transfected SH-SY5Y cells with the $CD8^{ED}$–$sorLA^{CD}$–WT construct in combination with sorLA–WT (Fig. 3*A*). The cells were subsequently stained with antibodies against the ED of sorLA and the CD8 reporter. As expected, we found a strong colocalization between $CD8^{ED}$–$sorLA^{CD}$–WT and sorLA–WT in a perinuclear Golgi-like compartment, demonstrating that the CD8 tag did not influence the subcellular distribution. Likewise, we found that $CD8^{ED}$–$sorLA^{CD}$–FANSHY→6A and sorLA–FANSHY→6A robustly overlapped albeit in a more peripherally localized compartment (Fig. 3*A*). Notably, when combining the mutant sorLA–FANSHY→6A with $CD8^{ED}$–$sorLA^{CD}$–WT, we observed only minor colocalization. Rather, the majority of sorLA–FANSHY→6A was observed in a peripheral and punctuate expression pattern (Fig. 3*B*). Transfection with the reverse constructs, i.e., $CD8^{ED}$–$sorLA^{CD}$–FANSHY→6A and sorLA–WT, showed a similar dispersed localization of the mutant receptor tail. In conclusion, sorLA–FANSHY→6A localize differently from sorLA–WT when transfected into the same cell.

Because our biochemical experiments suggested a critical role for the sequences $F^{9}TAF^{12}$ and $F^{12}ANSHY$ that share F^{12}, we compared the subcellular distribution of $CD8^{ED}$–$sorLA^{CD}$–WT with two mutants lacking either F^{9} and F^{12} (sorLA–FTAF→4A) or only F^{12} (sorLA–F^{12}→A) (compare with Fig. 2*A*). In accordance with the *in vitro* data, substitutions in sorLA–FTAF→4A, but also in sorLA–F^{12}→A, shifted the receptor distribution to the peripheral compartment similar to that observed for the sorLA–FANSHY→6A mutant (Fig. 3*C*). In comparison, mutating tyrosine 17 in FANSHY to a phenylalanine (sorLA-Y^{17}→F) did not influence the perinuclear expression pattern. Collectively, we therefore conclude that F^{12} in the receptor tail is important for retromer to control sorLA sorting.

To establish that the aberrant subcellular distribution of the mutants was a consequence of deficient retromer binding, we cotransfected the SH-SY5Y cells with the shRNA construct to knock down expression of VPS26. In the presence of functional retromer, $CD8^{ED}$–$sorLA^{CD}$–WT was confined to the perinuclear region, but transfection with the VPS26 shRNA clearly redistributed the receptor to a more distal and dispersed compartment in which it colocalized with the sorLA–FANSHY→6A mutant (Fig. 3*D*). These data strongly suggest a functional link between retromer, its binding to the FANSHY sequence, and sorting of sorLA.

Immunoelectron microscopy analysis of WT and mutant sorLA

To examine the protein localization in more detail, we performed immunoelectron microscopy on cells stably transfected with either sorLA–WT or sorLA–FANSHY→6A constructs. Unfortunately, despite several attempts, we did not succeed in generating a stable cell line that expressed sorLA–F^{12}→A. However, because the F^{12}→A and FANSHY→6A mutations had similar cellular localization patterns as shown in the CD8-reporter experiment (cf. Fig. 3*B*), all subsequent studies were performed using the FANSHY→6A mutant line. In agreement with the confocal IF data, immunoelectron microscopy revealed that sorLA–WT resides partly in Golgi compartments but also in large multivesicular bodies in the vicinity of the nucleus, whereas only small amounts of the WT receptor were present in peripheral compartments except for pronounced labeling of the plasma membrane (Fig. 3*E*). In contrast, the majority of sorLA–FANSHY→6A was

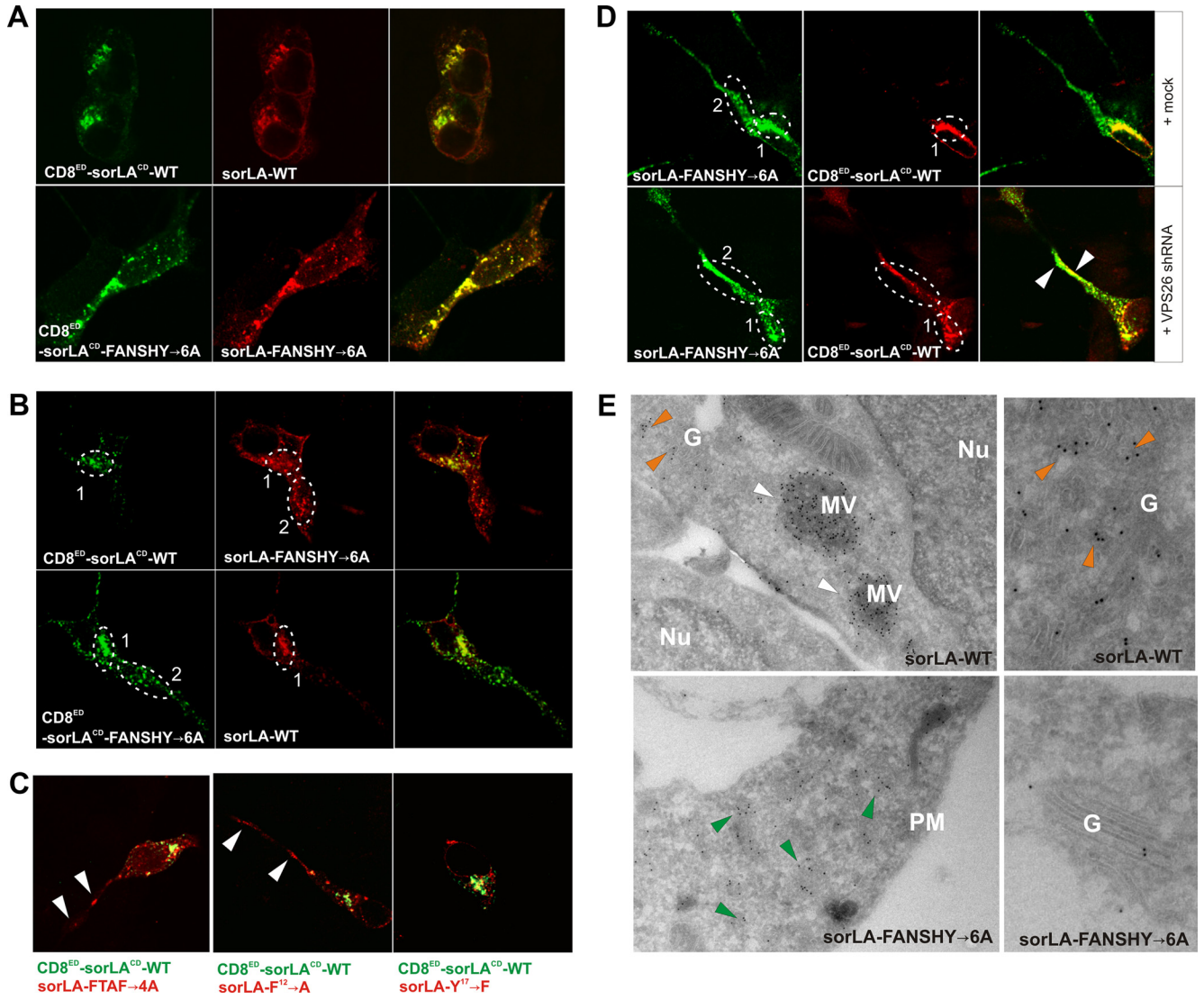

Figure 3. Mutation of the FANSHY motif changes the cellular localization of sorLA. ***A***, SH-SY5Y cells cotransfected with either CD8 ^{ED}–sorLA ^{CD}–WT and sorLA–WT (top) or CD8 ^{ED}–sorLA ^{CD}–FANSHY→6A and sorLA–FANSHY→6A (bottom) were stained for the extracellular domains of CD8 (green) or sorLA (red). ***B***, SH-SY5Y cells were transfected with a combination of constructs encoding either CD8 ^{ED}–sorLA ^{CD}–WT and sorLA–FANSHY→6A (top) or CD8 ^{ED}–sorLA ^{CD}–FANSHY→6A and sorLA–WT (bottom). The circled areas represent the perinuclear region and the more distal punctuate region (numbered 1 and 2), respectively. ***C***, Merged pictures of cotransfected SH-SY5Y cells with CD8 ^{ED}–sorLA ^{CD}–WT in combination with sorLA–FTAF→4A, sorLA-F ^{12}→A, or sorLA–Y ^{17}→F. Arrowheads indicate receptor localization in region 2. ***D***, SH-SY5Y cells were transfected with sorLA–FANSHY→6A and CD8 ^{ED}–sorLA ^{CD}–WT in either the absence (top) or presence (bottom) of the shRNA VPS26 knockdown vector. Arrowheads indicate colocalization in non-Golgi (non-perinuclear) compartments. ***E***, Electron microscopy analysis of sorLA–WT and sorLA–FANSHY→6A in the stably expressing SH-SY5Y cell lines. Arrowheads indicate receptor localization in multivesicular bodies (white), Golgi (orange), and peripheral vesicles (green). Nu, Nucleus; G, Golgi; MV, multivesicular bodies; PM, plasma membrane.

observed in small electron-dense vesicles near the plasma membrane but only to a small extent within the Golgi.

Reduced expression of sorLA–FANSHY→6A at the cell surface

The immunoelectron microscopy data also revealed low abundance of sorLA–FANSHY→6A at the plasma membrane when compared with the WT receptor (Fig. 4*A*). To quantitatively determine surface expression of the sorLA variants, we incubated the transfected SH-SY5Y cells with a membrane-impermeable biotin reagent at 4°C. A fraction of the total cell lysates and the biotinylated protein were resolved by SDS-PAGE analysis, and sorLA expression was determined by WB (Fig. 4*B*). Quantification of these bands demonstrated 48.3 ± 2.7% less sorLA–FANSHY→6A at the plasma membrane compared with the level of sorLA–WT.

We then speculated about whether the low cell-surface expression of sorLA–FANSHY→6A might be a consequence of deficits in the secretory pathway, leading to less mature receptor reaching the cell surface. To test this hypothesis, we examined receptor maturation using a pulse-chase protocol. The kinetics of receptor maturation (i.e., the acquisition of glycosylation) was indistinguishable between sorLA–WT and sorLA–FANSHY→6A as shown by a similar pattern of high and low glycosylated sorLA (Fig. 4*C*).

When sorLA reaches the plasma membrane, some receptor molecules can undergo cleavage by metalloproteases, leading to secretion of the soluble ED into the medium (Hampe et al., 2000). The time needed to reach the cell surface can be estimated by quantification of secreted soluble sorLA from the pulse-chase experiment. Accordingly, we immunoprecipitated newly synthesized and shed EDs from the cell culture medium at 60, 90, 120,

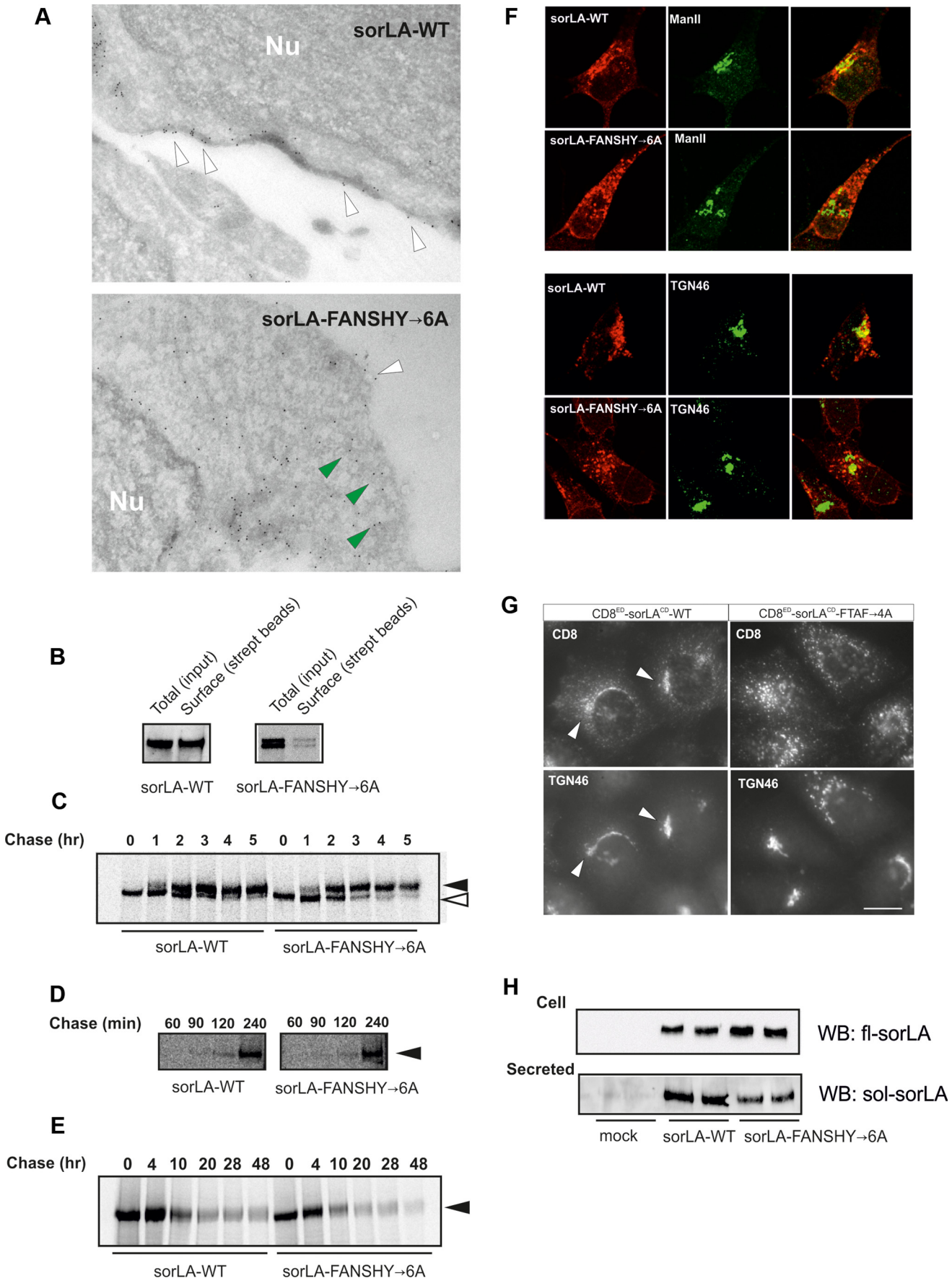

Figure 4. Characterization of sorLA transport in SH-SY5Y cell lines. ***A***, Immunoelectron microscopy of sorLA–WT and sorLA–FANSHY⟶6A. Nu, Nucleus. Arrowheads in white indicate surface labeling and mutant receptors in the vicinity of the plasma membrane by green arrowheads. ***B***, The level of biotinylated receptors at the cell surface (*Figure legend continues.*)

and 240 min after protein labeling. Neither the sorLA–WT nor sorLA–FANSHY→6A EDs were secreted after 60 min chase, but EDs from both proteins were secreted to a similar extent at later time points, i.e., 120 and 240 min (Fig. 4*D*). Together, these experiments suggest that anterograde transport of newly synthesized sorLA to the cell surface was not affected by mutation of the FANSHY motif in the cytoplasmic tail.

sorLA–FANSHY→6A mutant fails to enter the endosomal sorting pathway

We next investigated whether enhanced endocytic uptake and delivery to lysosomes for degradation might account for the impaired surface exposure of the sorLA–FANSHY→6A mutant. Accordingly, we metabolically labeled SH-SY5Y cells expressing either sorLA–WT or sorLA–FANSHY→6A for 40 min and chased proteins for the following 48 h. However, we failed to detect any major difference in turnover between the WT and mutant receptor (Fig. 4*E*). These data suggest that the mutant does not exhibit increased lysosomal targeting and degradation in SH-SY5Y cells (Fig. 4*E*).

The predominant expression of sorLA–FANSHY→6A in small electron-dense vesicles near the plasma membrane led us to suggest that the mutant might be impaired in retrograde trafficking from tubular endosomal network (TEN) and back to the Golgi, a pathway that is critically dependent on the retromer complex.

First, we studied colocalization of sorLA–WT and sorLA–FANSHY→6A with the Golgi markers ManII and TGN46 (Fig. 4*F*). Remarkably, we found only a modest overlap between sorLA–FANSHY→6A and ManII and TGN46, whereas sorLA–WT showed a much more pronounced colocalization (Fig. 4*F*) in line with the speculated defect in retrograde transport of the mutant.

Second, we used an antibody uptake protocol in which we labeled the chimeric proteins using an anti-CD8 antibody at the cell surface (Seaman, 2007) and studied internalization of the CD8^{ED}–sorLA^{CD}–WT and CD8^{ED}–sorLA^{CD}–FTAF→4A reporters in HeLa cells. In keeping with impaired retrograde trafficking, we found that antibody bound to CD8^{ED}–sorLA^{CD}–WT was endocytosed and delivered to the trans-Golgi compartment (TGN46-positive), whereas the CD8^{ED}–sorLA^{CD}–FTAF→4A fusion protein accumulated in punctate structures (Fig. 4*G*). A similar observation was made for the CD8^{ED}–sorLA^{CD}–FANSHY→6A reporter (data not shown), confirming that the aromatic motif is responsible for trans-Golgi network (TGN) retrieval.

In addition to mediating retrograde transport back to the Golgi, the TEN is also implicated in redirecting some receptor molecules back to the plasma membrane via recycling vesicles. If sorLA–FANSHY→6A accumulates within the tubular compartment as a result of deficient association with retromer, one could speculate that over time (steady-state) that less soluble sorLA would be released into the medium (as opposed to shedding of newly synthesized receptors; see the pulse-chase experiment in Fig. 4*D*). Despite almost identical expression of sorLA–WT and sorLA–FANSHY→6A in the stably transfected SH-SY5Y cells, we consistently detected ~30% less shedding of the mutant receptor when compared with the WT receptor ($p < 0.0001$) (Fig. 4*H*). These data suggest that recycling of sorLA–FANSHY→6A back to the cell surface is impaired. From these studies, we elaborate on a previously described model (Nielsen et al., 2007; Schmidt et al., 2007) in which sorLA moves through the secretory pathway to reach the cell surface. Our new studies suggest that, after internalization, sorLA is recycled back to the Golgi via the TEN—a sorting step that requires binding of VPS26 of the retromer complex to the FANSHY sequence in sorLA.

sorLA–FANSHY→6A interacts with APP

We have demonstrated previously that sorLA can bind to and retain APP in the Golgi compartment, thereby preventing processing of APP via both amyloidogenic and non-amyloidogenic pathways (Andersen et al., 2005; Schmidt et al., 2007). Because retromer deficiency increases the amyloidogenic degradation of APP (Small et al., 2005; Muhammad et al., 2008), we asked whether the sorLA–FANSHY→6A mutant might affect the subcellular localization and sorting of APP.

We first performed double-IF microscopy for sorLA–FANSHY→6A and APP in the transfected SH-SY5Y cells. The proteins exhibited a high degree of colocalization in the perinuclear region but notably also in the peripheral punctate structures (data not shown). This observation we corroborated using a PLA. In brief, an immunostaining was performed in which the secondary antibodies were tagged with oligonucleotides that can hybridize and be PCR amplified when antigens are within a distance of 40 nm. The resulting DNA strands were visualized by hybridization of fluorescently labeled oligonucleotides. Staining with the anti-sorLA and anti-APP antibodies generated a strong signal for both sorLA–WT and sorLA–FANSHY→6A (Fig. 5*A*). Notably, although the signal for sorLA–WT and APP was visible in a region close to the nucleus, it seemed that sorLA–FANSHY→6A and APP proximity was scattered throughout the cell, in line with the dispersed distribution of the mutant receptor (cf. Fig. 3*A*).

In additional experiments, we used FLIM to analyze the direct interaction of sorLA–WT and sorLA–FANSHY→6A with APP. In cells expressing APP alone, the lifetime of Alexa Fluor 488-labeled APP in the absence of acceptor Alexa Fluor 543-labeled sorLA was 2163 ± 127 ps ($n = 14$). This lifetime was shortened to 1979 ± 182 ps ($n = 15$; $p < 0.004$) in the presence of labeled sorLA. A similar reduction in the lifetime to 1982 ± 116 ps ($n = 13$; $p < 0.001$) was found for the APP-conjugated donor in the presence of sorLA–FANSHY→6A, indicating that mutation within the cytoplasmic domain of sorLA had little effect on the complex formation between sorLA and APP (Fig. 5*B*).

We conclude that retromer is required for trafficking of sorLA but not for formation of the sorLA:APP complex. Accordingly, the sorLA mutant devoid in retromer binding is able to redistribute APP to a compartment with a similar morphology to the TEN.

sorLA affects the trafficking of APP

Finally, we set out to investigate how sorLA–WT and sorLA–FANSHY→6A affect the vesicular transport of APP using time-

←

(*Figure legend continued.*) (streptavidin beads) relative to the total expression level (input) in SH-SY5Y cells shown by representative WB. ***C***, Pulse-chase experiment after the maturation of sorLA–WT and sorLA–FANSHY→6A in SH-SY5Y cells. Their glycosylation patterns are indicated by white (immature) and black (mature) arrowheads. ***D***, Pulse-chase experiment of secreted sorLA ectodomains. ***E***, Stability assay using pulse-chase technique. Proteins in ***C–E*** were visualized by radiography. ***F***, SH-SY5Y cells stably expressing sorLA–WT or sorLA–FANSHY→6A were stained for the receptor (in red) together with markers of Golgi (ManII) or TGN (TGN46) (in green). ***G***, Anti-CD8 antibody uptake in HeLa cells transfected with CD8^{ED}–sorLA^{CD}–WT or CD8^{ED}–sorLA^{CD}–FTAF→4A. Endosome-to-Golgi retrieval was evaluated by colocalization with TGN46. ***H***, Secretion of sorLA extracellular domains at steady state determined by WB analysis of 45 h conditioned medium (Secreted) from SH-SY5Y cells that express sorLA–WT or sorLA–FANSHY→6A (Cell).

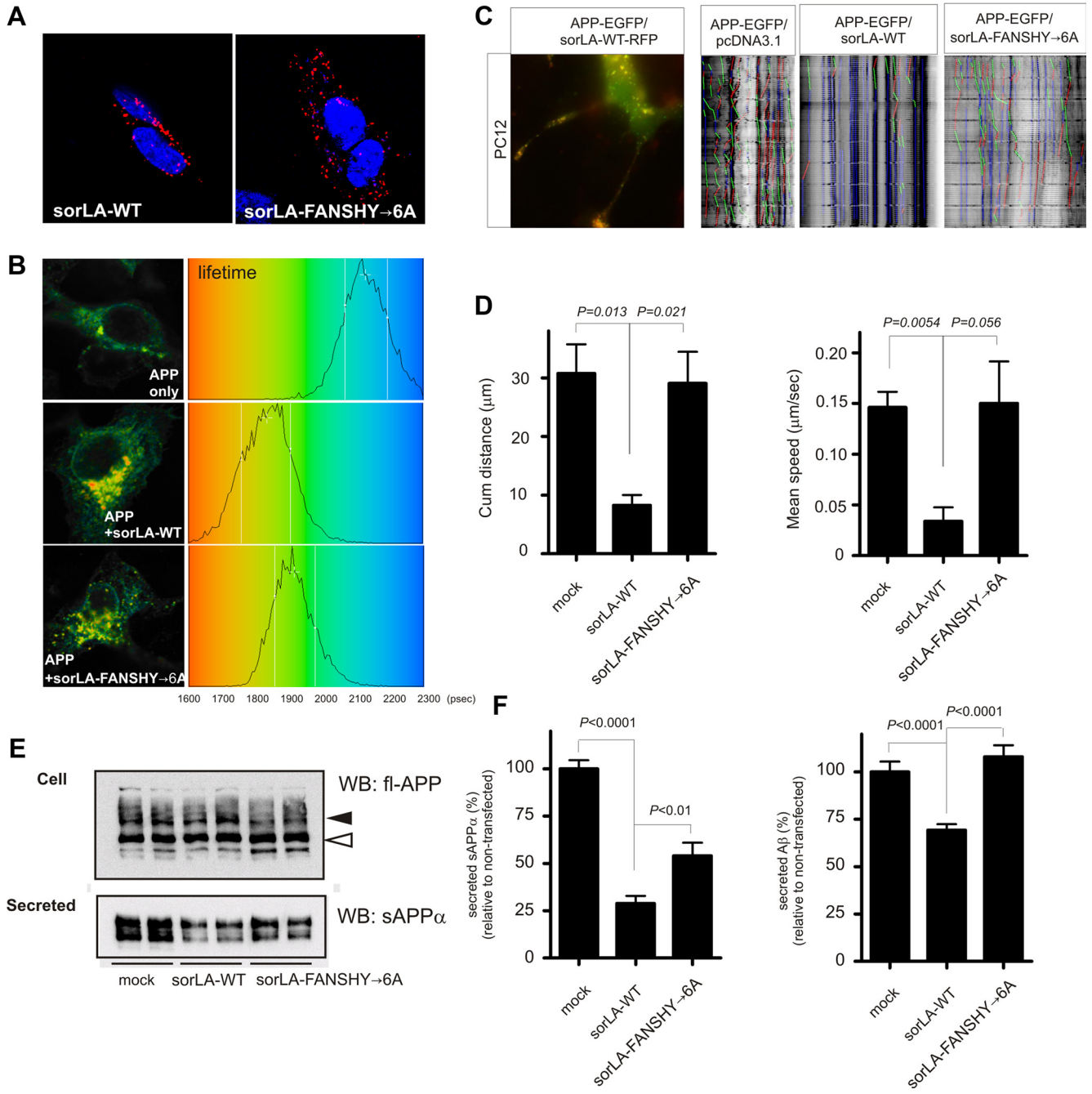

Figure 5. Binding of sorLA to retromer decreases APP transport and amyloidogenic processing. ***A***, PLA using SH-SY5Y cells stably expressing sorLA–WT or sorLA–FANSHY⟶6A and endogenous levels of APP. The red signal indicates protein–protein interactions between sorLA and APP. ***B***, FLIM analysis of the interaction between APP and sorLA–WT or sorLA–FANSHY⟶6A in SH-SY5Y cells. Shown are pseudocolored FLIM images (left) and lifetime histograms (right). ***C***, PC12 cells were transfected with APP–EGFP and sorLA–WT–RFP and differentiated by treatment with 50 ng/ml NGF to demonstrate colocalization between sorLA and APP in these cells. Vesicular movements were analyzed in PC12 cells, and representative kymographs from PC12 cells transfected with APP–EGFP in the absence of exogenous sorLA or cotransfected with sorLA–WT or sorLA–FANSHY⟶6A constructs are shown. Pausing vesicles are shown in blue, whereas vesicles moving anterograde and retrograde are colored in green and red, respectively. ***D***, Histograms showing the average mean speed for APP and the cumulative distance traveled by APP. Total number of vesicles analyzed per condition were as follows: APP, 354 vesicles; sorLA–WT, 226 vesicles; sorLA–FANSHY⟶6A, 287 vesicles. The vesicles were imaged over three experiments ($n = 3$), and the data are represented as mean ± SE. ***E***, APP metabolism in SH-SY5Y cells analyzed by WB of lysates (Cell) and conditioned medium (Secreted) of nontransfected cells and cells expressing either sorLA–WT or sorLA–FANSHY⟶6A. Mature and immature fl-APP (indicated by arrowheads) in the lysate was determined by antibody recognizing the C-terminal of full-length APP and secreted sAPPα was detected by the WO2 antibody. ***F***, Levels of sAPPα and Aβ in medium from SH-SY5Y cells determined by quantification of WB analysis or an Aβ_{40}-specific ELISA, respectively.

lapse imaging. Because previous studies had shown that sorLA–WT significantly reduces the velocity of the exit of a photo-activatable GFP–APP fusion protein from the perinuclear region (Schmidt et al., 2007), we studied whether sorLA–FANSHY⟶6A possesses a similar ability to reduce the speed of APP. We first transfected differentiated PC12 cells with APP–EGFP and sorLA–RFP constructs to validate that sorLA impairs APP trafficking. Not only did we observe a strong colocalization of sorLA–WT and APP within a subset of transport vesicles in the perinuclear region (Fig. 5*C*), we also noticed a strongly reduced velocity of vesicles containing both sorLA–RFP and APP–EGFP compared with vesicle containing only APP–EGFP (data not

shown). In a second round of experiments, we compared neurite dynamics of APP–EGFP alone or after cotransfection with either sorLA–WT or sorLA–FANSHY→6A. In the absence of sorLA expression, the majority of APP-containing vesicles were moving both retrogradely and anterogradely as shown by the kymograph (Fig. 5*C*). On the contrary, coexpression of sorLA–WT retarded transport of almost all APP-containing vesicles, reducing the cumulative distance traveled from 30.8 to 8.3 μm and the mean speed of vesicles from 0.15 to 0.03 μm/s (Fig. 5*D*). Remarkably, in the presence of sorLA–FANSHY→6A, movement of APP-containing vesicles were identical to the APP in mock-transfected cells.

These data suggest that sorLA only slows down APP trafficking if the receptor resides in the Golgi apparatus.

The sorLA–FANSHY→6A mutant does not protect against APP processing

We next compared the impact of sorLA–WT and sorLA–FANSHY→6A on APP processing. To do so, we first compared endogenous APP expression in parental SH-SY5Y with cell lines transfected with either one of the two sorLA constructs. WB of total cell lysates using an antibody against the C-terminal end of APP revealed that levels of immature and mature APP were not grossly affected by either sorLA–WT or sorLA–FANSHY→6A (Fig. 5*E*). However, when investigating shedding of soluble APP in medium collected for 48 h, we found a 71.2 ± 6.2% ($p < 0.0001$) reduction in secreted sAPPα in sorLA–WT-expressing cells. Interestingly, the sorLA–FANSHY→6A mutant was significantly less potent than the WT protein in preventing sAPPα processing (54.0 ± 7.0%; $p < 0.01$) compared with nontransfected cells (Fig. 5*F*).

Finally, we measured Aβ secretion using ELISA to determine the effect of the mutant receptor on the amyloidogenic processing pathway. By comparing the medium from nontransfected SH-SY5Y cells, we found a 30.8 ± 3.2% reduction ($p = 0.0001$) in Aβ production from cells that overexpress sorLA–WT. In contrast, sorLA–FANSHY→6A did not offer any protection against Aβ production, because the level of Aβ in the conditioned medium was not significantly different from nontransfected cells (Fig. 5*F*).

In conclusion, we have shown that sorLA is able to interact with retromer via VPS26 and this binding is necessary to retrieve to the Golgi complex. Aberrant sorLA trafficking by mutation in the FANSHY motif or loss of retromer function leads to altered APP processing and increased Aβ production. Our findings suggest a functional link between the impaired retromer expression observed in some cases of sporadic AD and the increase in amyloid burden.

Discussion

The precise sorting of APP during endocytosis is of critical importance for the AD pathology because Aβ generation (i.e., BACE cleavage) occurs in the acidic environment of the endosome. Besides endosomal sorting of APP, enlarged/dysfunctional endosomes have been implicated in AD progression, showing the importance of delineating sorting mechanisms of endosomal function (Nixon, 2005). This is supported by independent evidence that revealed altered expression of various sorting receptors and adaptors in AD (Small and Gandy, 2006).

In particular, defects in retromer-mediated transport have been linked to AD development. Studies combining brain imaging techniques with microarray analysis reported reduced expression of VPS35 and VPS26 in sporadic AD brains (Small et al., 2005). In addition, it has been proposed that retromer deficiency affects APP processing, thereby increasing Aβ levels (Small et al., 2005; Muhammad et al., 2008). Co-IP studies have indicated that retromer and APP exist in a multiprotein complex, although a direct interaction between APP and any of the retromer components has not yet been identified (Vieira et al., 2010).

sorLA is member of a group of membrane proteins including sortilin, CIMPR, and the iron transporter DMT1-II that undergo retromer-dependent transport from the endosomal compartments back to the Golgi. Recent studies have identified short peptide motifs required for retromer association. These motifs are highly hydrophobic and rich in aromatic amino acid residues, e.g., the tripeptides FLV (sortilin), WLM (CIMPR), and YLL (DMT1-II), respectively (Seaman, 2007; Tabuchi et al., 2010). However, up to now, the nature of the sorLA signal involved in retromer-dependent retrograde transport has not been elucidated (Bonifacino and Hurley, 2008). Here we demonstrate that retromer binds to an aromatic motif centered on F^{12} located in the FANSHY motif in the sorLA cytoplasmic tail. This observation is in accordance with the general view that retromer binding motifs contain aromatic residues. Interestingly, the binding of retromer to sortilin was mapped to the larger region of the sortilin cytoplasmic domain spanning the KKYVCGGR**F**LVHR**Y**SV-LQQHA sequence, containing the previously identified FLV tripeptide (Canuel et al., 2008). Therefore, we speculate that the separation between the two aromatic residues in this sequence (in bold) exactly corresponds to the **F**ANSH**Y** motif, suggesting that these two aromatic residues may define a common recognition motif for retromer within the family of mammalian VPS10 receptors.

Recognition of the FANSHY motif by retromer likely is mediated by the VPS26 subunit of the cargo-recognition VPS trimer. This is the first demonstration of a role for VPS26 in cargo binding and is consistent with the structural studies of VPS26 that revealed an arrestin-like conformation for the VPS26 protein and predicted a possible cargo-binding activity by analogy with the arrestin family of proteins (Shi et al., 2006; Collins et al., 2008). Although studies in both yeast and mammalian cells have indicated that VPS35 is responsible for the cargo-binding activity of retromer (Nothwehr et al., 2000; Arighi et al., 2004), our data suggest that this is not the case with respect to sorLA binding.

The role of the FANSHY motif in the sorLA cytoplasmic tail was investigated by mutagenesis. We found that sorLA–FANSHY→6A exhibits an altered cellular distribution to structures that were similar to the localization observed in cells lacking the retromer complex (Fig. 3*D*). In conclusion, mutating sorLA in the FANSHY motif or removing the retromer complex both lead to accumulation of the receptor in vesicular structures. The localization of sorLA–FANSHY→6A was clearly changed to a more vesicular structure that was positive for neither markers of TGN, late endosomes, nor lysosomes (data not shown). However, the observed pattern was similar to the localization of the retromer subunits VPS26 (Arighi et al., 2004), SNX1 (Carlton et al., 2004), and SNX2 (Carlton et al., 2005), which have been reported as tubules of the endosome, i.e., the TEN (Bonifacino and Rojas, 2006). A caveat to our study is that no specific markers for the TEN are yet known and that identification of the compartment solely relies on its morphological appearance. Obviously, this problem represents a significant challenge for future studies.

Therefore, we hypothesize that sorLA–FANSHY accumulates in the TEN, whereas sorLA–WT molecules can continuously undergo retromer-dependent retrograde transport back to the Golgi from the TEN (step 5; Fig. 6). Thus, the WT receptor can

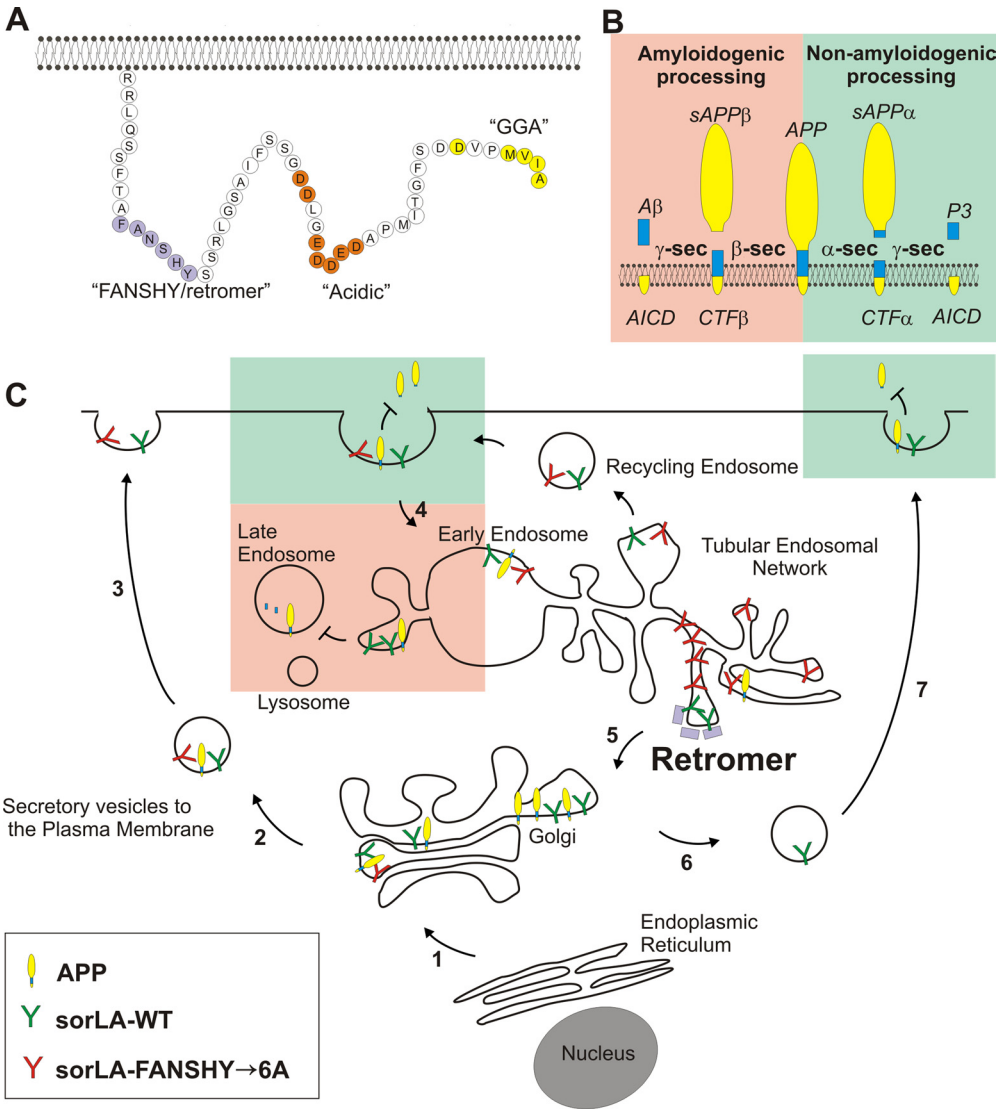

Figure 6. Model of the sorLA intracellular sorting pathways. ***A***, The amino acid sequence of sorLA including known binding sites for the specific cytosolic adaptor proteins retromer (FANSHY), PACS1/AP-2 (acidic sequence), and GGA (MVIA). ***B***, APP processing pathways. In the amyloidogenic pathway (red; to the left), APP is cleaved by β-secretase to generate sAPPβ and subsequent by γ-secretase to produce the Aβ peptide. In the non-amyloidogenic pathway (green; to the right), α-secretase cleaves within the Aβ sequence to generate sAPPα but inhibits amyloid production. ***C***, Schematic roadmap of the major transport pathways of WT and retromer-deficient binding sorLA in cells. Newly synthesized sorLA from ER traverses the Golgi en route to the plasma membrane in the secretory pathway independent of the FANSHY motif (steps 1–3). Both sorLA–WT and sorLA–FANSHY→6A are internalized from the cell surface (step 4) into the early endosome in which the receptors are sorted into distinct tubules of TEN (Andersen et al., 2005; Nielsen et al., 2007; Schmidt et al., 2007). Several pathways exist for exiting the TEN either into recycling endosomes going back to the cell surface or retrograde transport to the Golgi compartment depending on the different cytoplasmic coats surrounding individual tubules. We propose that the sorLA–FANSHY→6A mutant accumulates within SNX-coated tubules, being unable to associate with the cargo-specific VPS subunit of the retromer. In contrast, sorLA–WT is efficiently sorted back to the Golgi (step 5), leading to a higher steady-state level of sorting receptor (compared with the FANSHY→6A mutant) that also leads to higher levels at the cell surface (steps 6 and 7). APP is primarily localized in intracellular compartments, in which the interaction with sorLA–WT retains APP in the perinuclear compartments, leading to less shedding of sAPPα from the cell surface, and hinders entry to the amyloidogenic processing in the late endosomal pathway. sorLA–FANSHY→6A also in part inhibits APP degradation to sAPPα because of the initial localization at the plasma membrane, but there is very little receptor available to inhibit the amyloidogenic sorting into the late endosomes because this variant sorts into the TEN.

also be recycled to the plasma membrane to populate the cell surface more extensively than sorLA–FANSHY→6A as well as undergo secretion after cleavage, a process that also takes place at the cell surface (Fig. 6). Furthermore, our data suggest a model in which sorLA travels independently of retromer activity through the secretory pathway to the cell surface (steps 1–3). Also, endocytosis of sorLA by clathrin-coated pits into early/sorting endosomes (step 4) occurs independently of the retromer complex in line with previous findings that suggested that clathrin and retromer function in consecutive retrograde sorting steps (Popoff et al., 2007). This model is supported by a recent study describing a sorLA–F^{12}N^{14}Y^{17}→As mutant, which did not change the rate of internalization (Nielsen et al., 2007).

sorLA–WT is primarily localized within the Golgi and TGN, in which it functions as a retention factor for APP (Schmidt et al., 2007), resulting in less APP available for processing (Andersen et al., 2005; Offe et al., 2006). Therefore, a lack of sorLA retrieval from endosomes/TEN to the Golgi/TGN in the absence of retromer activity would lead to reduced sorLA binding to APP in the post-Golgi secretory pathway. Similarly, disrupting the interaction between sorLA and retromer by mutation of the FANSHY motif would also decrease the amount of sorLA in Golgi/TGN.

Hence, either the FANSHY mutation or the loss of retromer function will lead to a reduction of the Golgi/TGN localized sorLA and, consequently, increased APP trafficking to endosomal compartments. This mislocalization causes enhanced APP processing and increased Aβ levels. We believe that the removal of a functional interaction between sorLA and retromer by mutagenesis of the binding site represents an excellent model to study the importance of retromer-mediated APP transport compared with the retromer-deficient situation (Muhammad et al., 2008). The results of such studies may, however, be confounded by side effects from retromer acting on third-party proteins also involved in APP processing, e.g., BACE (He et al., 2005).

It is known that APP can be processed at the cell surface by α-secretase, whereas uncleaved molecules can internalize and undergo cleavage by β-secretase in the endocytic compartments. In cells that express sorLA–FANSHY→6A, we observed an increase in both sAPPα and Aβ levels, suggesting less protective receptor activity in the Golgi/TGN (loss of function) (Fig. 5). However, the increased expression of sorLA–FANSHY→6A within the endosomal system (gain of function) could alternatively associate with APP to reduce the exit of APP from the TEN, thereby enhancing the possibility of amyloidogenic cleavage within the acidic endosomal compartment. Also, a decrease of non-amyloidogenic cleavage at the cell surface could result from less APP trafficking from the TEN via recycling endosomes back to the plasma membrane. Currently, we are unable to distinguish between these two scenarios, and, in reality, both mechanisms could add to the observed differences. However, because sorLA–FANSHY→6A is also not able to lower the non-amyloidogenic processing, we believe that the reduced sorLA levels within the early compartments (loss of function) plays the major role in our model.

In conclusion, the present study identifies amino acid residues in the cytoplasmic domain of sorLA essential for the interaction with components of the retromer complex. We show that disruption of the FANSHY motif within sorLA leads to accumulation of the receptor in a distinct intracellullar compartment, most likely retromer-associated tubules of the TEN, which leads to increased Aβ production as seen in AD patients suffering from low expression levels of either sorLA or retromer.

References

Andersen OM, Christensen LL, Christensen PA, Sørensen ES, Jacobsen C, Moestrup SK, Etzerodt M, Thogersen HC (2000) Identification of the minimal functional unit in the low density lipoprotein receptor-related protein for binding the receptor-associated protein (RAP). J Biol Chem 275:21017–21024.

Andersen OM, Reiche J, Schmidt V, Gotthardt M, Spoelgen R, Behlke J, von Arnim CA, Breiderhoff T, Jansen P, Wu X, Bales KR, Cappai R, Masters CL, Gliemann J, Mufson EJ, Hyman BT, Paul SM, Nykjaer A, Willnow TE (2005) SorLA/LR11, a neuronal sorting receptor that regulates processing of the amyloid precursor protein. Proc Natl Acad Sci USA 102:13461–13466.

Andersen OM, Schmidt V, Spoelgen R, Gliemann J, Behlke J, Galatis D, McKinstry WJ, Parker MW, Masters CL, Hyman BT, Cappai R, Willnow TE (2006) Molecular dissection of the interaction between APP and its neuronal trafficking receptor SorLA/LR11. Biochemistry 45:2618–2628.

Arighi CN, Hartnell LM, Aguilar RC, Haft CR, Bonifacino JS (2004) Role of the mammalian retromer in sorting of the cation-independent mannose 6-phosphate receptor. J Cell Biol 165:123–133.

Bonifacino JS, Hurley JH (2008) Retromer. Curr Opin Cell Biol 20:427–436.

Bonifacino JS, Rojas R (2006) Retrograde transport from endosomes to the trans-Golgi network. Nat Rev Mol Cell Biol 7:568–579.

Canuel M, Lefrancois S, Zeng J, Morales CR (2008) AP-1 and retromer play opposite roles in the trafficking of sortilin between the Golgi apparatus and the lysosomes. Biochem Biophys Res Commun 366:724–730.

Carlton JG, Bujny MV, Peter BJ, Oorschot VM, Rutherford A, Arkell RS, Klumperman J, McMahon HT, Cullen PJ (2005) Sorting nexin-2 is associated with tubular elements of the early endosome, but is not essential for retromer-mediated endosome-to-TGN transport. J Cell Sci 118:4527–4539.

Carlton J, Bujny M, Peter BJ, Oorschot VM, Rutherford A, Mellor H, Klumperman J, McMahon HT, Cullen PJ (2004) Sorting nexin-1 mediates tubular endosome-to-TGN transport through coincidence sensing of high-curvature membranes and 3-phosphoinositides. Curr Biol 14:1791–1800.

Collins BM (2008) The structure and function of the retromer protein complex. Traffic 9:1811–1822.

Collins BM, Norwood SJ, Kerr MC, Mahony D, Seaman MN, Teasdale RD, Owen DJ (2008) Structure of Vps26B and mapping of its interaction with the retromer protein complex. Traffic 9:366–379.

Cramer JF, Gustafsen C, Behrens MA, Oliveira CL, Pedersen JS, Madsen P, Petersen CM, Thirup SS (2010) GGA autoinhibition revisited. Traffic 11:259–273.

Davis CG, Lehrman MA, Russell DW, Anderson RG, Brown MS, Goldstein JL (1986) The J.D. mutation in familial hypercholesterolemia: amino acid substitution in cytoplasmic domain impedes internalization of LDL receptors. Cell 45:15–24.

Dodson SE, Gearing M, Lippa CF, Montine TJ, Levey AI, Lah JJ (2006) LR11/SorLA expression Is reduced in sporadic Alzheimer disease but not in familial Alzheimer disease. J Neuropathol Exp Neurol 65:866–872.

Dodson SE, Andersen OM, Karmali V, Fritz JJ, Cheng D, Peng J, Levey AI, Willnow TE, Lah JJ (2008) Loss of LR11/SORLA enhances early pathology in a mouse model of amyloidosis: evidence for a proximal role in Alzheimer's disease. J Neurosci 28:12877–12886.

Haass C, Selkoe DJ (2007) Soluble protein oligomers in neurodegeneration: lessons from the Alzheimer's amyloid β-peptide. Nat Rev Mol Cell Biol 8:101–112.

Hampe W, Riedel IB, Lintzel J, Bader CO, Franke I, Schaller HC (2000) Ectodomain shedding, translocation and synthesis of SorLA are stimulated by its ligand head activator. J Cell Sci 113:4475–4485.

Harbour ME, Breusegem SY, Antrobus R, Freeman C, Reid E, Seaman MN (2010) The cargo-selective retromer complex is a recruiting hub for protein complexes that regulate endosomal tubule dynamics. J Cell Sci 123:3703–3717.

He X, Li F, Chang WP, Tang J (2005) GGA proteins mediate the recycling pathway of memapsin 2 (BACE). J Biol Chem 280:11696–11703.

Lane RF, Raines SM, Steele JW, Ehrlich ME, Lah JA, Small SA, Tanzi RE, Attie AD, Gandy S (2010) Diabetes-associated SorCS1 regulates Alzheimer's amyloid-β metabolism: evidence for involvement of SORL1 and the retromer complex. J Neurosci 30:13110–13115.

Lee JJ, Radice G, Perkins CP, Costantini F (1992) Identification and characterization of a novel, evolutionarily conserved gene disrupted by the murine Hb58 embryonic lethal transgene insertion. Development 115:277–288.

Motoi Y, Aizawa T, Haga S, Nakamura S, Namba Y, Ikeda K (1999) Neuronal localization of a novel mosaic apolipoprotein E receptor, LR11, in rat and human brain. Brain Res 833:209–215.

Muhammad A, Flores I, Zhang H, Yu R, Staniszewski A, Planel E, Herman M, Ho L, Kreber R, Honig LS, Ganetzky B, Duff K, Arancio O, Small SA (2008) Retromer deficiency observed in Alzheimer's disease causes hippocampal dysfunction, neurodegeneration, and Aβ accumulation. Proc Natl Acad Sci USA 105:7327–7332.

Nielsen MS, Madsen P, Christensen EI, Nykjaer A, Gliemann J, Kasper D, Pohlmann R, Petersen CM (2001) The sortilin cytoplasmic tail conveys Golgi-endosome transport and binds the VHS domain of the GGA2 sorting protein. EMBO J 20:2180–2190.

Nielsen MS, Gustafsen C, Madsen P, Nyengaard JR, Hermey G, Bakke O, Mari M, Schu P, Pohlmann R, Dennes A, Petersen CM (2007) Sorting by the cytoplasmic domain of the amyloid precursor protein binding receptor SorLA. Mol Cell Biol 27:6842–6851.

Nixon RA (2005) Endosome function and dysfunction in Alzheimer's disease and other neurodegenerative diseases. Neurobiol Aging 26:373–382.

Nothwehr SF, Ha SA, Bruinsma P (2000) Sorting of yeast membrane proteins into an endosome-to-Golgi pathway involves direct interaction of their cytosolic domains with Vps35p. J Cell Biol 151:297–310.

Offe K, Dodson SE, Shoemaker JT, Fritz JJ, Gearing M, Levey AI, Lah JJ (2006) The lipoprotein receptor LR11 regulates amyloid β production

and amyloid precursor protein traffic in endosomal compartments. J Neurosci 26:1596–1603.

Popoff V, Mardones GA, Tenza D, Rojas R, Lamaze C, Bonifacino JS, Raposo G, Johannes L (2007) The retromer complex and clathrin define an early endosomal retrograde exit site. J Cell Sci 120:2022–2031.

Reiche J, Theilig F, Rafiqi FH, Carlo AS, Militz D, Mutig K, Todiras M, Christensen EI, Ellison DH, Bader M, Nykjaer A, Bachmann S, Alessi D, Willnow TE (2010) SORLA/SORL1 functionally interacts with SPAK to control renal activation of Na^+-K^+-Cl^- cotransporter 2. Mol Cell Biol 30:3027–3037.

Rogaeva E, Meng Y, Lee JH, Gu Y, Kawarai T, Zou F, Katayama T, Baldwin CT, Cheng R, Hasegawa H, Chen F, Shibata N, Lunetta KL, Pardossi-Piquard R, Bohm C, Wakutani Y, Cupples LA, Cuenco KT, Green RC, Pinessi L, et al. (2007) The neuronal sortilin-related receptor SORL1 is genetically associated with Alzheimer disease. Nat Genet 39:168–177.

Rohe M, Carlo AS, Breyhan H, Sporbert A, Militz D, Schmidt V, Wozny C, Harmeier A, Erdmann B, Bales KR, Wolf S, Kempermann G, Paul SM, Schmitz D, Bayer TA, Willnow TE, Andersen OM (2008) Sortilin-related receptor with A-type repeats (SORLA) affects the amyloid precursor protein-dependent stimulation of ERK signaling and adult neurogenesis. J Biol Chem 283:14826–14834.

Sannerud R, Annaert W (2009) Trafficking, a key player in regulated intramembrane proteolysis. Semin Cell Dev Biol 20:183–190.

Scherzer CR, Offe K, Gearing M, Rees HD, Fang G, Heilman CJ, Schaller C, Bujo H, Levey AI, Lah JJ (2004) ApoE receptor LR11 in Alzheimer's disease: Gene profiling of lymphoblasts mirrors changes in the brain. Arch Neurol 61:1200–1205.

Schmidt V, Sporbert A, Rohe M, Reimer T, Rehm A, Andersen OM, Willnow TE (2007) SorLA/LR11 regulates processing of amyloid precursor protein via interaction with adaptors GGA and PACS-1. J Biol Chem 282:32956–32964.

Schwarz DG, Griffin CT, Schneider EA, Yee D, Magnuson T (2002) Genetic analysis of sorting nexins 1 and 2 reveals a redundant and essential function in mice. Mol Biol Cell 13:3588–3600.

Seaman MN (2004) Cargo-selective endosomal sorting for retrieval to the Golgi requires retromer. J Cell Biol 165:111–122.

Seaman MN (2005) Recycle your receptors with retromer. Trends Cell Biol 15:68–75.

Seaman MN (2007) Identification of a novel conserved sorting motif required for retromer-mediated endosome-to-TGN retrieval. J Cell Sci 120:2378–2389.

Seaman MN (2008) Endosome protein sorting: motifs and machinery. Cell Mol Life Sci 65:2842–2858.

Seaman MN, Marcusson EG, Cereghino JL, Emr SD (1997) Endosome to Golgi retrieval of the vacuolar protein sorting receptor, Vps10p, requires the function of the VPS29, VPS30, and VPS35 gene products. J Cell Biol 137:79–92.

Seaman MN, McCaffery JM, Emr SD (1998) A membrane coat complex essential for endosome-to-Golgi retrograde transport in yeast. J Cell Biol 142:665–681.

Shi H, Rojas R, Bonifacino JS, Hurley JH (2006) The retromer subunit Vps26 has an arrestin fold and binds Vps35 through its C-terminal domain. Nat Struct Mol Biol 13:540–548.

Skinner CF, Seaman MN (2009) The role of retromer in neurodegenerative disease. In: Intracellular traffic and neurodegenerative disorders (St. George-Hyslop P, ed), pp 125–140. Heidelberg: Springer.

Small SA, Gandy S (2006) Sorting through the cell biology of Alzheimer's disease: intracellular pathways to pathogenesis. Neuron 52:15–31.

Small SA, Kent K, Pierce A, Leung C, Kang MS, Okada H, Honig L, Vonsattel JP, Kim TW (2005) Model-guided microarray implicates the retromer complex in Alzheimer's disease. Ann Neurol 58:909–919.

Söderberg O, Gullberg M, Jarvius M, Ridderstråle K, Leuchowius KJ, Jarvius J, Wester K, Hydbring P, Bahram F, Larsson LG, Landegren U (2006) Direct observation of individual endogenous protein complexes in situ by proximity ligation. Nat Methods 3:995–1000.

Tabuchi M, Yanatori I, Kawai Y, Kishi F (2010) Retromer-mediated direct sorting is required for proper endosomal recycling of the mammalian iron transporter DMT1. J Cell Sci 123:756–766.

Vieira SI, Rebelo S, Esselmann H, Wiltfang J, Lah J, Lane R, Small SA, Gandy S, da Cruz ESEF, da Cruz E Silva OA (2010) Retrieval of the Alzheimer's amyloid precursor protein from the endosome to the TGN is S655 phosphorylation state-dependent and retromer-mediated. Mol Neurodegener 5:40.

Wassmer T, Attar N, Bujny MV, Oakley J, Traer CJ, Cullen PJ (2007) A loss-of-function screen reveals SNX5 and SNX6 as potential components of the mammalian retromer. J Cell Sci 120:45–54.

Willnow TE, Petersen CM, Nykjaer A (2008) VPS10P-domain receptors: regulators of neuronal viability and function. Nat Rev Neurosci 9:899–909.